Critical slowing down and entanglement protection

Eliana Fiorelli,[1,2,3,4] Alessandro Cuccoli,[1,2] and Paola Verrucchi[5,1,2]
[1]*Dipartimento di Fisica e Astronomia, Università di Firenze, 50019 Sesto Fiorentino, Italy*
[2]*INFN, Sezione di Firenze, 50019 Sesto Fiorentino, Italy*
[3]*School of Physics and Astronomy, University of Nottingham, Nottingham NG7 2RD, United Kingdom*
[4]*Centre for the Mathematics and Theoretical Physics of Quantum Non-equilibrium Systems, University of Nottingham, Nottingham NG7 2RD, United Kingdom*
[5]*ISC, CNR, UOS Dipartimento di Fisica, Università di Firenze, 50019 Sesto Fiorentino, Italy*

(Received 6 February 2019; published 26 September 2019)

We consider a quantum device D interacting with a quantum many-body environment R which features a second-order phase transition at $T = 0$. Exploiting the description of the critical slowing down undergone by R according to the Kibble-Zurek mechanism, we explore the possibility to freeze the environment in a configuration such that its impact on the device is significantly reduced. Within this framework, we focus on the magnetic-domain formation typical of the critical behavior in spin models and propose a strategy that allows one to protect the entanglement between different components of D from the detrimental effects of the environment.

DOI: 10.1103/PhysRevA.100.032123

I. INTRODUCTION

In recent decades studies on how to manipulate quantum systems have boosted the scientific community's confidence in regard to the possible realization of quantum devices. These are usable apparatuses whose operating principles are based on genuinely quantum properties, among which entanglement between components is key to outperforming classical machines. Given that an apparatus is usable if some external control can be exerted on the state and evolution of its components, the description of a quantum device must envisage the existence of at least another system, which enforces such control by interacting with the device itself. This means that a quantum device is open to the external world by definition, and it is not a stretch to name "environment" whatever influences its behavior from the outside. For this reason, the analysis of how quantum devices work implies the study of how open quantum systems evolve [1–9].

In fact, it is one of the most challenging tasks of quantum technologies, that of allowing quantum devices to be "open" and yet to properly function [10]: Quantum properties are fragile and vulnerable to the environmental impact, and strategies for their protection [11–21] most often imply either the suppression of the interaction between the environment and device (which is never exactly achievable) or a very detailed design of their couplings (which is usually an experimentally arduous task).

In this work we aim at understanding if a quantum device D can be protected by intervening in some properties of its environment R, without quenching the interaction between D and R or giving it too peculiar a form. To this aim, we specifically consider the case when R is a quantum many-body system featuring a second-order phase transition and investigate the possible consequences of a critical behavior of R on the entanglement between different components of D. The reason for this choice is the possible exploitation of the critical slowing down leading to the Kibble-Zurek mechanism (KZM) in order to freeze the environment in a configuration that is as harmless as possible for the device.

In order to focus this argument, we first notice that any entanglement between D and R (hereafter dubbed external) is useless as far as the device functioning is concerned, and its buildup inevitably goes with damages of that between different components of D (hereafter dubbed internal), which is the useful one. A naive strategy for protecting the latter by minimizing the former is to deal with an environment that behaves almost classically [22], which is to say it can only be weakly entangled with any other system. Referring to the case of a magnetic environment, which is what we will hereafter do, an almost-classical R can be obtained in the form of a system with a large value of the spin $\mathcal{S}$ [23]; however, the effect of one such system upon each component of D could be so prevalent as to squash the fragile quantum machineries that make the device function, up to the point of making its state always separable, as if its components were not part of a unique composite system D.

We therefore propose another strategy, based on the magnetic-domain formation which is typical of the critical behavior of many spin models. In fact, each domain is a large-$\mathcal{S}$ system and yet different domains do not point in the same direction, which should result in an overall weaker effect of R on the device components. Moreover, the dynamics of magnetic domains can be significantly slowed down in the vicinity of a second-order phase transition, which might also help protect the internal entanglement.

The paper is organized as follows. In Sec. II we define the model of the quantum device and its environment, with Secs. II A and II B devoted to a brief description of the critical slowing down and the Kibble-Zurek mechanism, respectively. In Sec. III we introduce the tools used in Secs. IV and V to study the evolution of the overall model. The dynamics of the entanglement between the device components is described in

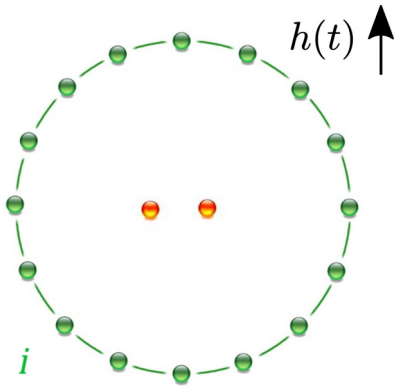

FIG. 1. Schematic representation of the ring of spins with a central qubit pair.

Sec. VI. Our results are presented and discussed in Sec. VII. A summary is given and conclusions are drawn in Sec. VIII.

II. MODEL

We consider a device-plus-environment quantum system $\Psi = D + R$, where the device is a qubit pair $D = A + B$ and the environment is a ring R, made of N spin-$\frac{1}{2}$ particles, as shown in Fig. 1. Each qubit is described by the Pauli operators $\hat{\boldsymbol{\sigma}}_*$, with $[\hat{\sigma}_*^\alpha, \hat{\sigma}_*^\beta] = i2\epsilon_{\alpha\beta\gamma}\hat{\sigma}_*^\gamma$, $\alpha(\beta, \gamma) = x, y, z$, and $* = A, B$, while elements of R are described by operators $\hat{\mathbf{s}}_i$, with $[\hat{s}_i^\alpha, \hat{s}_j^\beta] = i\epsilon_{\alpha\beta\gamma}\delta_{ij}\hat{s}_i^\gamma$, $|\hat{\mathbf{s}}_i|^2 = \frac{3}{4}$, $i(j) = 1, \ldots, N$, and periodic boundary conditions enforced, $\hat{\mathbf{s}}_{N+1} = \hat{\mathbf{s}}_1$.

As we want R to feature a second-order phase transition that survives the lowering of temperature (so that we can reduce the thermal effects without modifying our setting), we focus on quantum phase transitions (QPTs), which are second-order phase transitions occurring at zero temperature, under the tuning of some model parameter. In this respect notice, however, that quantum critical properties survive at sufficiently low and yet finite temperatures, which makes the following analysis amenable to experimental investigation. The $N \to \infty$ limit underlying the occurrence of any genuine phase transition is implemented by combining a large value of N with the periodic boundary conditions inherent in the ring geometry.

In the above general framework we specifically choose R to be described by a prototypical spin model for a one-dimensional QPT. As for the two qubits, they are coupled with each component of the ring via a ZX ferromagnetic exchange but do not interact among themselves and they are not subject to the transverse field that drives the QPT. We will comment on these choices in Sec. VIII.

The dimensionless Hamiltonian of the system is

$$\hat{H} = \hat{H}_{\rm I} - \frac{g}{2}\left(\hat{\sigma}_A^z + \hat{\sigma}_B^z\right)\sum_{i=1}^{N}(\hat{s}_i^+ + \hat{s}_i^-), \tag{1}$$

with

$$\hat{H}_{\rm I} = -\sum_{i=1}^{N}\hat{s}_i^x\hat{s}_{i+1}^x - h(t)\sum_{i=1}^{N}\hat{s}_i^z \tag{2}$$

the Hamiltonian of the ring, where we have chosen a ferromagnetic Ising interaction whose exchange integral J sets the energy scale (i.e., the physical Hamiltonian of the model is the above dimensionless one times the actual exchange integral J). The coupling g is positive, and $h(t)$ accounts for the presence of a time-dependent transverse (i.e., pointing in the $+z$ direction) magnetic field that drives the QPT. We will also consider the case of constant field.

As for the initial state of the system, we will take it to be separable as far as the partition $D + R$ is concerned,

$$|\Psi(0)\rangle = |D\rangle \otimes |R\rangle, \tag{3}$$

where the state of the qubit pair is

$$|D\rangle = \sum_\gamma c_\gamma\,|\gamma\rangle, \tag{4}$$

with $\{|\gamma\rangle\}_{\mathcal{H}_D}$ the four eigenstates of $(\hat{\sigma}_A^z + \hat{\sigma}_B^z)$, generically labeled by the index $\gamma = 1, \ldots, 4$; the coefficients c_γ are complex numbers and are different from zero for at least two different γ, in order to ensure that A and B are entangled.

A. Critical behavior of the ring

The Hamiltonian $\hat{H}_{\rm I}$ defines the one-dimensional quantum Ising model in a transverse field (QIF), which is a paradigmatic example of a system undergoing a QPT [24]. The transition occurs due to the competition between the action of the external field, which supports independent alignment of each spin in the z direction, and the exchange coupling among adjacent spins, which favors their being parallel to each other and all pointing in the x direction. The control parameter driving the transition is the field h, with the QPT located at $h = 1$; the region where critical behaviors are observed is usually dubbed the critical region. For the sake of clarity, in this section we will use the parameter

$$\epsilon := h - 1 \tag{5}$$

and set the QPT at $\epsilon_c = 0$.

The order parameter for the QIF is the x component of the magnetization

$$\frac{1}{N}\sum_j \langle\hat{s}_j^x\rangle = \langle\hat{s}_i^x\rangle \equiv m\,\forall\, i, \tag{6}$$

where by $\langle\cdot\rangle$ we indicate the expectation value on the translationally invariant ground state; m is finite in the ordered phase ($\epsilon < 0$) and it vanishes in the disordered one ($\epsilon > 0$). In the critical region, the related correlation functions $\chi_r := \langle\hat{s}_i^x\hat{s}_{i+r}^x\rangle$ behave according to

$$\chi_r - m^2 \sim e^{-r/\xi}, \tag{7}$$

where ξ is the correlation length, which diverges at the transition as

$$\xi \sim \frac{\xi_0}{|\epsilon|^\nu}, \tag{8}$$

with $\nu > 0$ the corresponding critical exponent and ξ_0 a nonuniversal length scale. We notice that ξ is sometimes dubbed the healing length, to indicate that it sets the scale upon which $\langle\hat{s}_i^x\rangle$ heals in space, returning to the spatially homogeneous value m after having been affected by a local fluctuation. A similar concept can be introduced to describe the way the system reacts to instantaneous, i.e., local in time,

fluctuations. This leads to the introduction of a quantity called relaxation, or reaction, time τ, which sets the timescale upon which the relevant quantities settle, after the control parameter has varied instantaneously. The reaction time is also known to diverge at the transition, according to

$$\tau \sim \frac{\tau_0}{|\epsilon|^{\nu z}}, \tag{9}$$

with $z > 0$ the so-called dynamical critical exponent and τ_0 a nonuniversal timescale. It is worth mentioning that the product νz also rules the critical vanishing of the gap Δ between the ground-state energy and that of the first-excited one, $\Delta \sim |\epsilon|^{\nu z}$, signaling the most relevant relation between such vanishing and the occurrence of the QPT itself. Without further commenting on this point, which has been extensively discussed in the literature, let us specifically address Eq. (9).

A divergent relaxation time implies an extremely slow dynamics of the system as a whole, with fast fluctuations occurring only locally without any significant effect on the global scale set by the correlation length. This phenomenon, which is usually referred to as a critical slowing down, is evidently intertwined with the divergence of the correlation length, if only for the fact that both Eqs. (8) and (9) describe a power-law divergence at $\epsilon = \epsilon_c = 0$. On the other hand, a finite relaxation time is key to the definition of adiabaticity, i.e., the distinctive feature of dynamical regimes where the system changes its state (or configuration, in the classical case), after the variation of relevant parameters, in a time interval that is much shorter than the timescale of the variation itself. Therefore, we expect the divergence of τ at $\epsilon = 0$, as well as the consequent critical slowing down, to be related to the onset of a nonadiabatic regime, sometimes called diabatic, which is indeed at the heart of the KZM described below.

B. Kibble-Zurek mechanism

An exact analytical description of the dynamical evolution of a many-body quantum system which is driven across its phase transition is an unattainable task, for the very same reason that the transition occurs, i.e., the presence of terms in the system Hamiltonian that do not commute, not even at different times. From a numerical viewpoint, the situation is equivalently intractable, even in a classical system, because of several divergences that characterize any critical behavior. However, in the same spirit that allows one to derive and use equations such as Eqs. (8) and (9), it is possible to elaborate on criticality to get an effective description of the process through which a phase transition dynamically happens. This is how Kibble and Zurek built a paradigm to describe out-of-equilibrium dynamics around a continuous phase transition, today known as the Kibble-Zurek mechanism. The theory was initially proposed by Kibble [25] within the cosmological context, later extended by Zurek [26,27] to condensed-matter systems, and finally extended to QPTs [28–33]. The mechanism takes different forms depending on the model Hamiltonian and the functional time dependence of the control parameter.

In this section we describe the KZM for the QIF when the transverse field varies linearly in time,

$$h(t) = h_0 - vt, \tag{10}$$

with positive velocity v; $1/v$ is referred to as the quench time, suggesting that the transition is crossed by lowering the field, i.e., moving from the disordered to the ordered phase. In fact, this is the process to which we will refer in this work, with $h_0 > 1$ to set the model in the disordered phase when the process starts.

The control parameter in Eq. (5) is

$$\epsilon(t) = h(t) - 1 = (h_0 - 1) - vt, \tag{11}$$

which embodies the definition of a critical time

$$t_c = \frac{h_0 - 1}{v} \tag{12}$$

after which the QPT is reached; more generally, the time left before the transition is crossed is

$$\delta(t) = t_c - t = \frac{h_0 - 1}{v} - t. \tag{13}$$

The key observation leading to the KZM is that, due to the divergence of the reaction time (9), there certainly exists a finite time interval where

$$\delta(t) \leqslant \tau, \tag{14}$$

meaning that before the system has reacted globally to the control-parameter variation, the critical point has already been reached, a situation which is evidently inconsistent with any adiabaticlike dynamics. In fact, if Eq. (14) holds, the system cannot merely adapt to the variation of the control parameter but rather gets stuck on a configuration that is qualitatively the one taken when $\delta(t) = \tau$, i.e., at the time

$$\bar{t} = \frac{h_0 - 1}{v} - \sqrt{\frac{1}{2v}}, \tag{15}$$

where we have used Eqs. (9) and (11) with $\nu = z = 1$ and $\tau_0 = \frac{1}{2}$, which are the expected values for the QIF.

From the above description, the diabatic dynamical regime is set in the time interval

$$\bar{t} \leqslant t \leqslant 2t_c - \bar{t}. \tag{16}$$

The aforesaid process can be graphically depicted as in Fig. 2. The magenta line represents the reaction time τ that diverges at t_c, when $\epsilon(t_c) = 0$ and the critical point is reached. The purple line is $\delta(t)$ as from Eq. (13), while the blue one is $\epsilon(t)$ from Eq. (11). The shaded area is where $\delta(t) \leqslant \tau$.

In fact, the KZM goes beyond the above phenomenology and describes its implications as far as the dynamics of the system is concerned. In the remaining part of this section, we discuss these implications for the QIF in the disordered phase, aimed at devising approximations to be used in the diabatic regime.

Referring to the process as represented in Fig. 2, we know that for large fields, despite the ring being in its disordered phase as far as the spin correlations in the x direction are concerned, its ground state is ordered, with all the spins aligned in the z direction, though independent of each other. Consistently with the usual terminology, we will understand that in the disordered noncritical phase, the ring exhibits a paramagnetic behavior.

Once the quench starts the dynamics is still adiabatic, with the magnetization in the z direction that decreases with

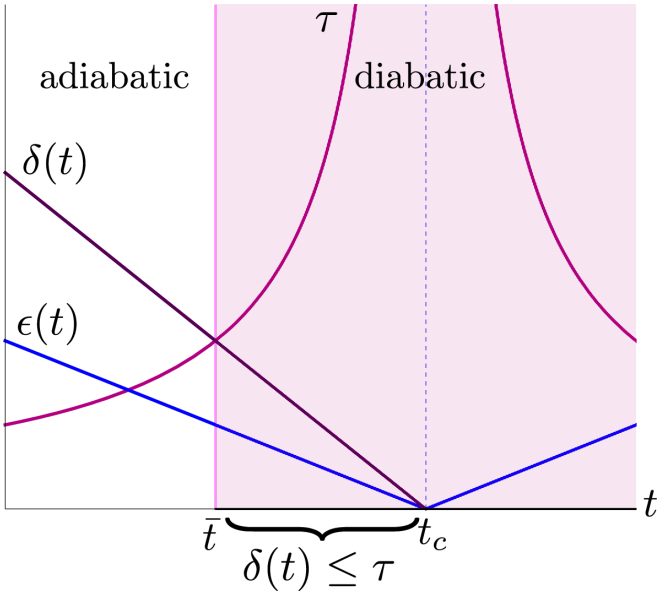

FIG. 2. Schematic representation of the KZM. See the text below Eq. (16) for a detailed description.

time, as long as the reaction time is smaller than $\delta(t)$, i.e., for $t \lesssim \bar{t}$. However, blocks of dynamically correlated spins, hereafter dubbed domains, begin to appear. If the exponential behavior (7) has already set in, a correlation length exists and it makes sense to take the length of the above domains to be of the same order of magnitude.

When the QPT gets closer and the reaction time becomes much longer than $\delta(t)$, i.e., for $t \gtrsim \bar{t}$, adiabaticity is lost: The ring has no time to conform its state to the instantaneous ground state of the time-dependent Hamiltonian and it gets stuck in the state where it was at $t = \bar{t}$, with domains of average length $\xi[\epsilon(\bar{t})] := \xi_d$. Due to the homogeneity of the Ising coupling along the ring, these domains require a time which is proportional to ξ_d to establish dynamical correlations among themselves. On the other hand, at $t = \bar{t}$ the system is in its critical region, meaning that ξ_d is very large. Therefore, different domains cannot be causally connected and can be effectively described as noninteracting. This is a relevant point in Sec. V, where the formation of effectively noninteracting domains allows us to describe R in terms of large independent spins.

C. Weak-coupling constraint

The phenomenology described in Secs. II A and II B refers to the ring as if it were not interacting with the two qubits, i.e., as if $g = 0$ in the Hamiltonian (1). On the other hand, we aim at exploiting the KZM to control the dynamics of the complete model, with $g > 0$.

This is made possible by enforcing a weak-coupling constraint

$$g \ll 1, \quad g \ll h(t) \tag{17}$$

throughout the rest of this work. These conditions have no implication on the description of the critical behavior, which occurs when $|h(t)| \sim 1$, but they definitely rule out the region where the ring becomes effectively ordered due to the vanishing of $h(t)$. Therefore, to avoid inconsistencies with respect to this point, our analysis will exclusively concern the disordered phase $h(t) \geqslant 1$, where the conditions (17) can be safely assumed. This will be used in Secs. IV and V, in order to get an effective propagator and hence the evolved state of the system, in both the paramagnetic and diabatic settings.

III. STRATEGY AND ESSENTIAL TOOLBOX

In this section we explain our goal and provide the reader with the essential tools we have used to accomplish it. Referring to the possible strategies to protect the internal entanglement mentioned in the Introduction, we will compare the way the entanglement between A and B decreases after the interaction with R is switched on, in two different settings, both relative to the disordered $\epsilon > 0$ phase.

First, we will consider the dynamics of the model for a constant large value of h so as to set the ring far from its critical region; in this case we expect it to behave as an almost classical paramagnet, acting upon D as if it were one single system with a very large spin $\mathcal{S}$, pointing in the direction of the field. The overall evolution of the system will be effectively ruled by the coupling between D and R only, and we will refer to this setting as the paramagnetic case.

Second, we will set the ring well within the critical region and drive it into the diabatic regime by quenching the magnetic field as $h(t) = h_0 - vt$, with $h_0 \gtrsim 1$. The time dependence of the field will enter the evolution of the system (with the KZM playing an essential role in effectively describing it), and we will refer to this setting as the diabatic case.

In both settings we will study how the initial state (3) changes under the action of the propagator defined by the Hamiltonian (1); this will allow us to obtain the evolved state of D (a mixed state due to the generation of external entanglement) via the partial trace over the Hilbert space of R; the internal entanglement dynamics will be finally analyzed in terms of the time dependence of the concurrence [34] between the two qubits. Despite the peculiar features of the paramagnetic and diabatic regimes, the coupling between R and D makes it impossible to exactly determine the evolution of the state (3). This is due to the commutation rules obeyed by spin operators, which most often prevent one from getting closed factorized expressions for the propagators by the Zassenhaus formula [35], i.e., the dual of the Baker-Campbell-Hausdorff one. However, when dealing with spin operators describing a system with a large value of $\mathcal{S}$, we can obtain a reasonable approximation by the following argument.

Hamiltonians that contain terms $g\hat{S}^\alpha$, with g some coupling constant as in Eq. (1), can be considered in the large-$\mathcal{S}$ limit provided g scales as $\frac{1}{\mathcal{S}}$, so as to keep the corresponding energy finite. Such a condition turns into $g\mathcal{S} \sim$ const or, quite equivalently,

$$g^m \mathcal{S}^\ell \sim 0 \, \forall \, m > \ell \geqslant 1; \tag{18}$$

this is how we will hereafter enforce the large-$\mathcal{S}$ condition whenever needed. Notice that, according to these conditions, the weak-coupling constraint $0 < g \ll 1$, introduced in Sec. II C, corresponds to taking $1 \ll \mathcal{S} < \infty$. Moreover, the above reasoning also applies if the large-$\mathcal{S}$ spin operators

$\hat{S}^\alpha$ enter the propagator further multiplied by other operators acting on the Hilbert space of a different physical subsystem, with which they therefore inherently commute, such as the qubit operators $\hat{\sigma}^z_{A,B}$ in the second term of Eq. (1).

In the following two sections we will factorize the propagator $\exp\{-it\hat{H}\}$ by the Zassenhaus formula for spin operators (see Appendix A), possibly with large $\mathcal{S}$, and apply it to the initial state (3), with $|R\rangle$ described by spin-$\mathcal{S}$coherent states (CSs) that are described in Appendix B.

IV. PARAMAGNETIC CASE

In this section we consider the dynamics of the overall model at $T = 0$, in the weak-coupling regime, for a constant value of the field. Such a value is understood to be sufficiently large to guarantee an approximately paramagnetic behavior of R in the absence of D.

A. Initial state

Consistently with the ring behaving as a paramagnet, we choose its initial state as

$$|\mathcal{R}\rangle = \otimes_{i=1}^{N} |\uparrow_i\rangle, \tag{19}$$

where $|\uparrow_i\rangle$ is the eigenstate of $\hat{s}^z_i$ with eigenvalue $\frac{1}{2}$. In fact, we will adopt a description in terms of spin-$\frac{1}{2}$ CSs (see Appendix B) identifying each $|\uparrow_i\rangle$ with the reference state $|0_i\rangle$ used to define the spin-$\frac{1}{2}$ CSs for the particle sitting at site i. For the sake of clarity, these spin-$\frac{1}{2}$ CSs will be hereafter indicated by $|\omega_i\rangle$. We therefore write the initial state of the system in the paramagnetic case as

$$|\Psi_{\text{para}}(0)\rangle = |D\rangle \otimes_{i=1}^{N} |\omega_i = 0\rangle. \tag{20}$$

B. Propagator

We handle the propagator via the Zassenhaus formula (A5) with $\lambda = -it$ and $\hat{X} = \hat{H}_{\text{I}}$. This implies that $\hat{Y}$ is proportional to g, and we can implement the weak-coupling constraint (17) by only taking terms in Eq. (A2) which are linear in g, thus getting

$$C_{n+1} = \frac{g}{2}\frac{(\hat{\sigma}^z_A + \hat{\sigma}^z_B)h^n}{(n+1)!}\sum_i [(-1)^{n+1}\hat{s}^+_i - \hat{s}^-_i]. \tag{21}$$

By carefully manipulating the factors of the Zassenhaus formula, we get

$$e^{-it\hat{H}}_{\text{para}} \simeq \left[\prod_{i=1}^{N} \exp\left(\frac{\hat{\sigma}^z_A + \hat{\sigma}^z_B}{2}[l(t)\hat{s}^-_i - l(t)^*\hat{s}^+_i]\right)\right] e^{-it\hat{H}_I}, \tag{22}$$

with

$$l(t) = \frac{g}{h}(1 - e^{-ith}). \tag{23}$$

C. Evolved state

The evolved state is obtained by acting with the propagator (22) on the initial state (20). In fact, the form of the above propagator dictates to first evaluate the action of $e^{-it\hat{H}_I}$ on the initial state of the ring. As we are in the paramagnetic case, the state (19) is a good approximation of the ground state of $\hat{H}_I$ with energy $E_{\text{g.s.}}$; therefore, the second factor on the right-hand side of Eq. (22) gives rise to an irrelevant overall phase factor $\exp\{-itE_{\text{g.s.}}\}$ that we will hereafter drop. We thus find

$$|\Psi_{\text{para}}(t)\rangle = \sum_\gamma c_\gamma |\gamma\rangle \left(\otimes_{i=1}^{N} e^{\pi_\gamma[l(t)\hat{s}^-_i - l(t)^*\hat{s}^+_i]}|0_i\rangle\right), \tag{24}$$

where π_γ are the eigenvalues of $(\hat{\sigma}^z_A + \hat{\sigma}^z_B)/2$. As each exponential in this expression is the displacement operator [see Eq. (B1)] for one spin of the ring acting on the respective reference state, it is

$$|\Psi_{\text{para}}(t)\rangle = \sum_\gamma c_\gamma \ \otimes_{i=1}^{N} |\omega^\gamma(t)\rangle_i \tag{25}$$

for

$$\omega^\gamma(t) = \pi_\gamma l(t) \tag{26}$$

and $l(t)$ as in Eq. (23).

V. DIABATIC CASE

In this section we study the dynamical process underlying our proposal for protecting internal entanglement by the critical slowing down implied by the KZM. We recall that we now consider the model in the weak-coupling regime, with a time-dependent field $h(t) = h_0 - vt$, and $h_0 \gtrsim 1$ so as to set R in its disordered critical region, where domains of dynamically correlated spins exist according to the phenomenology described in Sec. II. If the ring has already entered the diabatic region $t > \bar{t}$, these domains are effectively noninteracting and frozen in size, their length being on the order of $\xi_d := \xi[\epsilon(\bar{t})]$, which is the same as saying that each domain involves ξ_d adjacent spins of the ring, given the dimensionless character of all our expressions. Since R is made of N spins, the number of distinct domains is $n_d = N/\xi_d$.

Spins within the same domain stay roughly aligned with each other by definition. Therefore, the internal dynamics of each domain can be neglected, and the evolution of R can be described in terms of spin operators relative to distinct domains. In other terms, one can replace the notion of a domain as a set of ξ_d spin-$\frac{1}{2}$ particles with that of a single spin-$\mathcal{S}_d$ system, with $\mathcal{S}_d \sim \xi_d/2$. Formally, this is done by defining the collective spin operators $\hat{\mathbf{S}} := \sum_{i=1}^{\xi_d} \hat{\mathbf{s}}_i$, such that $|\hat{\mathbf{S}}|^2 = \mathcal{S}_d(\mathcal{S}_d + 1)$, so that the whole ring can be described by a set of n_d spin operators $\{\hat{\mathbf{S}}_\delta\}$, with $\delta = 1, \ldots, n_d$, each describing a spin-$\mathcal{S}_d$ system, with the same $\mathcal{S}_d \sim \xi_d/2$, as depicted in Fig. 3.

Once the above description is adopted, the original exchange interaction in Eq. (2) is mapped into the effective one

$$-j_{\text{eff}} \sum_{\delta=1}^{n_d} \hat{S}^x_\delta \hat{S}^x_{\delta+1}, \tag{27}$$

with a dimensionless coupling j_{eff} which is determined according to the following reasoning. Given the nearest-neighbor nature of the original Ising exchange, its contribution from one single domain is $\sim\xi_d/4$ and from the whole ring is $\sim n_d\xi_d/4 = N/4$, i.e., a constant that can be safely neglected. This means that the total exchange energy of the original

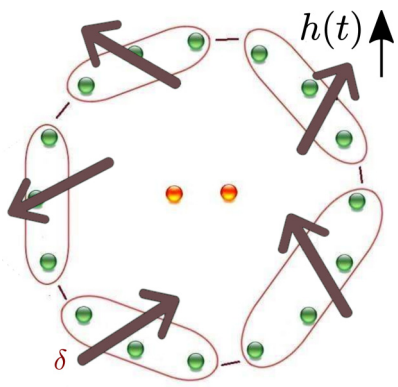

FIG. 3. Schematic representation of the spins S_j with the central qubit pair.

model must equal the interaction energy between neighboring spins on the edge of adjacent domains, i.e., $j_{\rm eff} n_d \mathcal{S}_d^2 m^2 \simeq n_d m^2$, where we have written $\langle \hat{s}_i^x \hat{s}_{i+1}^x \rangle$ as m^2 by Eq. (7) with $r = 1$ and $\xi \gg 1$. In fact, as we are in the disordered critical region, it is $m = 0$; however, the above reasoning works regardless of what side of the QPT is considered, and we can safely use it to determine how $j_{\rm eff}$ scales with the domain size. Finally, recalling that $\mathcal{S}_d \sim \xi_d/2$, we get

$$j_{\rm eff} \sim \frac{2}{\xi_d^2} \ll 1. \tag{28}$$

The strong reduction of the Ising coupling between domains represented by Eq. (28) is consistent with the KZM picture of approximately noninteracting domains and allows us to neglect the Ising term in Eq. (2) and write the effective Hamiltonian in the diabatic setting as

$$\hat{H}_{\rm dia}(t) \simeq -h(t) \sum_{\delta=1}^{n_d} \hat{S}_\delta^z - \frac{g}{2}\left(\hat{\sigma}_A^z + \hat{\sigma}_B^z\right) \sum_{\delta=1}^{n_d} (\hat{S}_\delta^+ + \hat{S}_\delta^-). \tag{29}$$

It is worth noting that all the operators $\{|\hat{\mathbf{S}}_\delta|^2\}$ commute with $\hat{H}_{\rm dia}(t)$ at any time, which formally confirms our considering $\mathcal{S}_d$ fixed.

A. Initial state of the ring (diabatic)

Consistently with the above picture, we take the initial state of the ring as

$$|\mathcal{R}_{\rm dia}\rangle = \otimes_{\delta=1}^{n_d} |\Delta_\delta\rangle, \tag{30}$$

where $|\Delta_\delta\rangle$ is the initial state of the δth domain, which is determined by the following reasoning. The KZM implies that each domain behaves as a spin-$\mathcal{S}_d$ system, with $\mathcal{S}_d \gg 1$: Given the large value of $\mathcal{S}_d$, one can resort to a semiclassical picture and say that each domain points in some direction $\mathbf{n}_\delta(0) := \mathbf{n}(\vartheta_\delta(0), \varphi_\delta(0))$, where $\mathbf{n}(\vartheta, \varphi) = (\sin\vartheta\cos\varphi, \sin\vartheta\sin\varphi, \cos\vartheta)$ is the unit vector along the direction defined by the spherical polar angles (ϑ, φ). On the other hand, there exist quantum spin-$\mathcal{S}$ states which are in one-to-one correspondence with unit vectors in $\mathbb{R}^3$ and that formally transform into those vectors in the $\mathcal{S} \to \infty$ limit; they are the spin-$\mathcal{S}$ CSs introduced in Appendix B. Therefore, it makes sense to choose

$$|\Delta_\delta\rangle = |\Omega_\delta(0)\rangle = e^{\Omega_\delta(0)\hat{S}_\delta^- - [\Omega_\delta(0)]^* \hat{S}_\delta^+} |0_\delta\rangle, \tag{31}$$

where $\Omega_\delta(0)$ is in one-to-one correspondence with the above direction $\mathbf{n}_\delta(0)$ via Eq. (B3). As for the choice of the set of initial domain directions, i.e., of the n_d parameters $\{\Omega_\delta(0)\}$, we have used a specific procedure to make it consistent with the expected value of the ring magnetization along the z direction, as described in Appendix C.

B. Propagator (diabatic)

The Hamiltonian in the diabatic setting is inherently time dependent, meaning that, at variance with the paramagnetic case considered in Sec. IV, the propagator embodies a troublesome time-ordering operator. However, since $[H_{\rm dia}(t_1), H_{\rm dia}(t_2)] \sim v(t_1 - t_2)/\mathcal{S}_d$ and we are dealing with extended domains ($\mathcal{S}_d \gg 1$), the propagator can still be written as $\exp\{-it\hat{H}_{\rm dia}(t)\}$ as long as vt is not too large, which is guaranteed, via Eq. (11), by the diabatic setting, $h_0 \gtrsim 1$ and $\epsilon(t) > 0$.

Therefore, we can again handle the propagator via the Zassenhaus formula (A5) with $\lambda = -it$, now setting $\hat{X} = -h_t \sum_\delta^{n_d} \hat{S}_\delta^z$, and $\hat{Y} = -\frac{g}{2}(\hat{\sigma}_A^z + \hat{\sigma}_B^z) \sum_\delta^{n_d} (\hat{S}_\delta^+ + \hat{S}_\delta^-)$, where $h_t := h(t)$ for the sake of simpler notation. Since $\mathcal{S}_d \gg 1$ we use the approximation (18) and get

$$\begin{aligned} C_{n+1} &\sim \frac{(-1)^n}{(n+1)!}(it)^{n+1} h_t^n \frac{g}{2}\left(\hat{\sigma}_A^z + \hat{\sigma}_B^z\right) \\ &\quad \times \sum_\delta \big[\underbrace{\hat{S}_\delta^z, \ldots, \hat{S}_\delta^z}_{n \text{ times}}, \hat{S}_\delta^+ + \hat{S}_\delta^-\big] \ldots \big] \\ &= \begin{cases} \dfrac{(it)^{n+1}}{(n+1)!} h_t^n \dfrac{g}{2}\left(\hat{\sigma}_A^z + \hat{\sigma}_B^z\right) \displaystyle\sum_\delta (\hat{S}_\delta^+ + \hat{S}_\delta^-) & \text{if } n \text{ is even} \\ \dfrac{(it)^{n+1}}{(n+1)!} h_t^n \dfrac{g}{2}\left(\hat{\sigma}_A^z + \hat{\sigma}_B^z\right) \displaystyle\sum_\delta (\hat{S}_\delta^+ - \hat{S}_\delta^-) & \text{if } n \text{ is odd.} \end{cases} \end{aligned} \tag{32}$$

By carefully manipulating the factors of the Zassenhaus formula, we obtain

$$e_{\rm dia}^{-it\hat{H}} \sim \prod_\delta e^{ith_t \hat{S}_\delta^z} e^{[(\hat{\sigma}_A^z + \hat{\sigma}_B^z)/2][f(t)\hat{S}_\delta^- - f^*(t)\hat{S}_\delta^+]}, \tag{33}$$

with

$$f(t) = \frac{g}{h_t}(e^{ith_t} - 1). \tag{34}$$

C. Evolved state (diabatic)

Under the effect of the above propagator, the initial state (3), with $|R\rangle$ as from Eqs. (30) and (31), evolves into

$$|\Psi_{\rm dia}(t)\rangle = \sum_\gamma c_\gamma |\gamma\rangle \otimes_\delta e^{ith_t \hat{S}_\delta^z} e^{\pi_\gamma [f(t)\hat{S}_\delta^- - f(t)^* \hat{S}_\delta^+]} |\Omega_\delta(0)\rangle, \tag{35}$$

where π_γ are the eigenvalues of $(\hat{\sigma}_A^z + \hat{\sigma}_B^z)/2$. To evaluate the action of the propagator on the initial state, we first note that

$$e^{\pi_\gamma [f(t)\hat{S}_\delta^- - f(t)^* \hat{S}_\delta^+]} = e^{\Omega^\gamma(t)\hat{S}_\delta^- - [\Omega^\gamma(t)]^* \hat{S}_\delta^+} = \hat{\Omega}_\delta^\gamma(t), \tag{36}$$

with $\Omega^\gamma(t) := \pi_\gamma f(t)$, i.e., via Eq. (B2),

$$\vartheta^\gamma(t) = \frac{g|\pi_\gamma|2\sqrt{2}}{h_t}\sqrt{1-\cos(th_t)},$$
$$\varphi^\gamma(t) = \arctan\left(\frac{\pi_\gamma g}{h_t}[\cos(th_t)-1], \frac{\pi_\gamma g}{h_t}\sin(th_t)\right). \quad (37)$$

Then, using the composition rule (B10) and the definition (31), we obtain

$$\hat{\Omega}^\gamma_\delta(t)\,|\Omega_\delta(0)\rangle = |\Omega^\gamma_\delta(t)\rangle\, e^{i\Phi^\gamma_\delta(t)\mathcal{S}_d}, \quad (38)$$

with $\Phi^\gamma_\delta(t) = \Phi(\Omega^\gamma(t), \Omega_\delta(0)) \in \mathbb{R}$, and

$$\mathbf{n}^\gamma_\delta(t) = \mathbf{R}_{\Omega^\gamma(t)}\mathbf{n}_\delta(0), \quad (39)$$

with $\mathbf{R}_{\Omega^\gamma(t)}$ the rotation in $\mathbb{R}^3$ defined in Eq. (B5). The final state thus reads

$$|\Psi_{\rm dia}(t)\rangle = \sum_\gamma c_\gamma\,|\gamma\rangle \otimes_\delta e^{i\Phi^\gamma_\delta(t)\mathcal{S}_d} e^{ith_t\hat{S}^z_\delta}\left|\Omega^\gamma_\delta(t)\right\rangle. \quad (40)$$

The further action of the exponential containing $\hat{S}^z_\delta$ can be made explicit via the decomposition (B8) of the spin-$\mathcal{S}$ CSs on the eigenstates of $\hat{S}^z$ reported in Appendix B. However, as this is irrelevant in what follows, we keep the state $|\Psi_{\rm dia}(t)\rangle$ as it is in Eq. (40).

VI. ENTANGLEMENT EVOLUTION

In this section we focus upon the internal entanglement featured by the evolved states in the paramagnetic and diabatic setting, Eqs. (25) and (40), respectively. We first notice that in both cases it is

$$|\Psi(t)\rangle = \sum_\gamma c_\gamma\,|\gamma\rangle\,|R^\gamma(t)\rangle, \quad (41)$$

and hence, by partially tracing $|\Psi(t)\rangle\langle\Psi(t)|$ upon the Hilbert space of the ring, the state of the device reads

$$\rho_D(t) = \sum_{\gamma\gamma'}(c_\gamma c^*_{\gamma'}\,|\gamma\rangle\langle\gamma'|)\,\langle R^{\gamma'}(t)|R^\gamma(t)\rangle, \quad (42)$$

with

$$\langle R^{\gamma'}(t)|R^\gamma(t)\rangle_{\rm para} = \prod_{i=1}^N \left\langle\omega^{\gamma'}_i(t)\middle|\omega^\gamma_i(t)\right\rangle \quad (43)$$

in the paramagnetic case and

$$\langle R^{\gamma'}(t)|R^\gamma(t)\rangle_{\rm dia} = \prod_\delta^{n_d} e^{i[\Phi^\gamma_\delta(t)-\Phi^{\gamma'}_\delta(t)]\mathcal{S}_d}\left\langle\Omega^{\gamma'}_\delta(t)\middle|\Omega^\gamma_\delta(t)\right\rangle \quad (44)$$

in the diabatic one.

To proceed with a quantitative analysis, we must choose a specific initial state for the device, and we go for

$$|D\rangle = \frac{1}{\sqrt{2}}(|00\rangle + |11\rangle), \quad (45)$$

which is a maximally entangled state. This implies that in all our formulas γ takes just two values, hereafter labeled by $+$ and $-$, corresponding to $\pi_\pm = \pm 1$. Moreover, we have to evaluate the overlaps between coherent states entering Eqs. (43) and (44), which we do by means of Eq. (B6).

Finally, a comparison between the time dependence of the internal entanglement in the paramagnetic and diabatic settings can be developed in terms of the concurrence $C_{AB}(\rho)$ between A and B relative to the state $\rho_D(t)$ in the two cases. Using Eq. (25), in the paramagnetic setting we find

$$C^{\rm para}_{AB}[\rho_D(t)] = \max\left\{0, \cos\left(\frac{\Theta(t)}{2}\right)^N\right\}, \quad (46)$$

where

$$\cos[\Theta(t)] := \cos\theta^+(t)\cos\theta^-(t) + \sin\theta^+(t)\sin\theta^-(t)\cos[\phi^+(t)-\phi^-(t)], \quad (47)$$

with $(\theta^\pm(t), \phi^\pm(t))$ such that $\omega^\pm(t) = \frac{\theta}{2}e^{i\phi}$ and $\omega^\pm(t)$ from Eq. (26). Using Eq. (40), in the diabatic setting we get

$$C^{\rm dia}_{AB}[\rho_D(t)] = \max\left\{0, \left[\prod_{\delta=1}^{n_d}\cos\left(\frac{\Theta_\delta(t)}{2}\right)\right]^{2\mathcal{S}_d}\right\}, \quad (48)$$

with

$$\cos[\Theta_\delta(t)] := \cos\vartheta^+_\delta(t)\cos\vartheta^-_\delta(t) + \sin\vartheta^+_\delta(t)\sin\vartheta^-_\delta(t)\cos[\varphi^+_\delta(t)-\varphi^-_\delta(t)], \quad (49)$$

and $(\vartheta^\pm_\delta(t), \varphi^\pm_\delta)$ from Eqs. (39) and (B3).

VII. RESULTS

In this section we present and discuss our results, Eqs. (46) and (48), for the time dependence of the entanglement between the qubits A and B, due to their interaction with the magnetic environment R. We recall that the form (33) used to obtain Eq. (48) holds when the ring is in its diabatic region, i.e., for $t > \bar{t}$. Therefore, in what follows we describe a dynamical process that starts at a time $t_0 > \bar{t}$ and show our numerical data versus the interval $t - t_0$. Regarding the interaction, a weak-coupling constraint is enforced via the condition (18), meaning that, in order to keep the interaction between R and D finite, we consider domains of large but finite size.

The following analysis is carried out by comparing the evolution of the concurrence C_{AB} in the paramagnetic and the diabatic settings, with $C_{AB}(t_0) = 1$ due to our choice of preparing D in the maximally entangled state (45). This comparison is complicated by the fact that, besides the common parameters N and g, other parameters can be independently varied within the same setting so that different values of the magnetic field can be considered in the paramagnetic case, independently of the choice of different quench velocities and initial magnetic fields in the diabatic one. Therefore, for the sake of clarity, we first compare results for the two settings and then consider different realizations of the diabatic one. In this part of the analysis we set $N = 120$ and $g = 0.15$ (which ensures that the weak-coupling condition holds); at the end of the section, however, we also consider the difference between the time dependence of C_{AB} in the two settings as a function

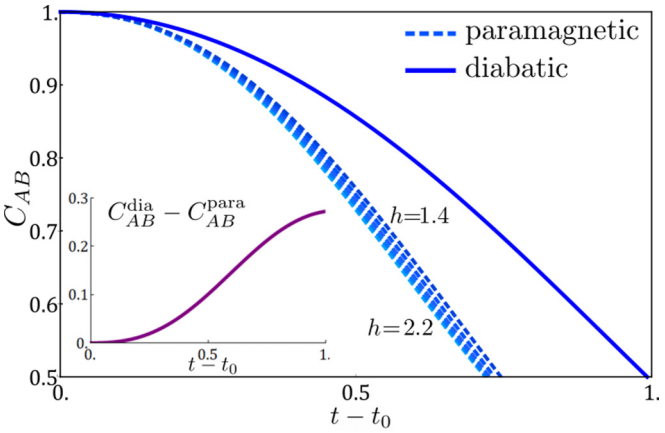

FIG. 4. Plot of C_{AB} vs $t - t_0$. The solid line shows the diabatic setting with $h_0 = 1.01$, $v = 0.6 \times 10^{-3}$, and $t_0 = \bar{t} + 12$. The dashed line shows the paramagnetic setting with h ranging from 1.4 to 2.2 in steps of 0.2. The inset shows the difference between data in the two different settings, with $h = 2$ in the paramagnetic one. The other parameters are $N = 120$ and $g = 0.15$.

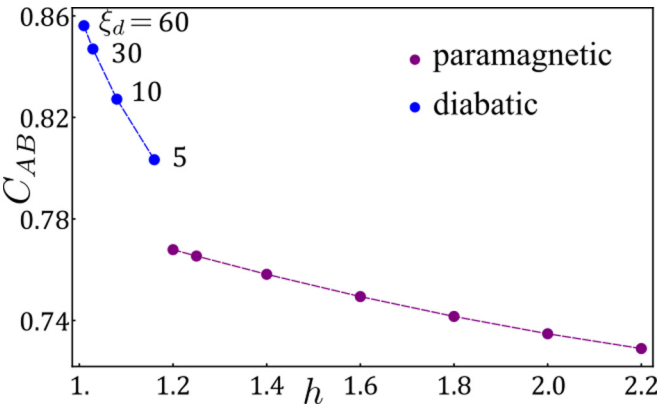

FIG. 5. Plot of C_{AB} vs h at time $\tilde{t} = 0.5 + t_0$. The purple circles show the paramagnetic setting. The blue circles show the diabatic setting with the domain size as indicated and $t_0 = \bar{t} + 12$ for $\xi_d = 60$, $t_0 = \bar{t} + 1.5$ for $\xi_d = 30$, $t_0 = \bar{t} + 0.5$ for $\xi_d = 10$, and $t_0 = \bar{t} + 0.1$ for $\xi_d = 5$. Lines are guides for the eyes. The other parameters are $N = 120$ and $g = 0.15$.

of g and for $N = 1000$. As for the constant ξ_0 entering Eq. (8), it will be hereafter set equal to 1.

Let us start by comparing the time dependence of the concurrence in paramagnetic settings with different values of the field,with that observed in the simplest nontrivial diabatic setting (namely, that where R is effectively described by just two independent domains, of size $N/2$). Data are shown in Fig. 4 for $t - t_0 \in [0, 1]$. The paramagnetic curves are obtained for values of the field from $h = 1.4$ to $h = 2.2$, in steps of 0.2. The diabatic curve is for $h_0 = 1.01$, $v = 0.6 \times 10^{-3}$, $t_0 = \bar{t} + 12$, and $n_d = 2$.

The decline of the concurrence is evidently slower in the diabatic setting. However, such a decline is seen to slow down with the lowering of h and, given that the diabatic curve corresponds to the lowest value of the field, one might argue that decreasing the field is a way to reduce the detrimental effect of the environment *per se*. Aiming at better insight on this point, in Fig. 5 we plot C_{AB} at a specific time $\tilde{t} = 0.5 + t_0$ as a function of h; these data show that there actually is a relevant difference between the way C_{AB} behaves in the paramagnetic setting (purple circles) and in the diabatic one (blue circles), with the transition towards the second one implying a much better performance as far as the entanglement protection is concerned. This confirms that the KZM allows one to maintain higher values of the concurrence due to the formation and substantial freezing of noninteracting large-$\mathcal{S}$ domains in the ring.

In order to further highlight the role played by the specific features of the domains, let us briefly recall the idea behind our strategy. We expect the entanglement protection to emerge when (i) R splits into macroscopic and independent domains with large S and (ii) the disentangling effect that such domains exert on D, by inducing a magnetic alignment of A and B separately, vanishes on average, due to the domains being uncorrelated and their magnetic moments consequently pointing in different directions. On the other hand, while macroscopicity in (i) requires a small number of domains, the vanishing of the net magnetic effect in (ii) is more likely when such a number is large, and it is hard to say whether a better protection is obtained by giving priority to one or the other mechanism. Note that this is not a moot point, since the number of domains depends on the quench velocity, which is an external parameter that can be chosen to control the overall dynamics. In fact, recalling the phenomenology described in Sec. II B, it is easily seen that diabatic settings with different quench velocities drive the very same R into effective systems with a different number of domains. Specifically, as the speed v decreases, R splits into a decreasing number of larger domains.

Returning to Fig. 5, the data suggest that a lower number of domains of larger size should be preferred. To check if this is a general result, in Fig. 6 we show the time dependence of C_{AB} for different values of the quench velocity, $v = 0.6 \times 10^{-3}, 2.2 \times 10^{-3}, 20 \times 10^{-3}$, corresponding to R being

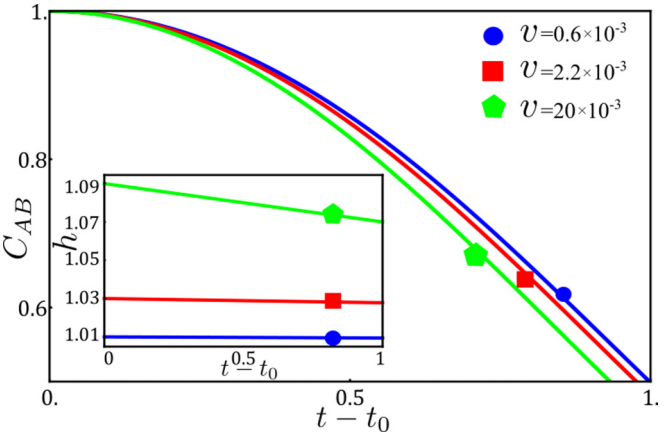

FIG. 6. Plot of C_{AB} vs $t - t_0$ in different diabatic settings. The blue curve shows $v = 0.6 \times 10^{-3}$, $h_0 = 1.01$, $t_0 = \bar{t} + 12$, and $\xi_d = 60$. The red curve shows $v = 2.2 \times 10^{-3}$, $h_0 = 1.03$, $t_0 = \bar{t} + 1.5$, and $\xi_d = 30$. The green curve shows $v = 20 \times 10^{-3}$, $h_0 = 1.09$, $t_0 = \bar{t} + 0.5$, and $\xi_d = 10$. The other parameters are $N = 120$ and $g = 0.15$. The inset shows the corresponding time dependence of the applied field, $h = h_0 - v(t - t_0)$.

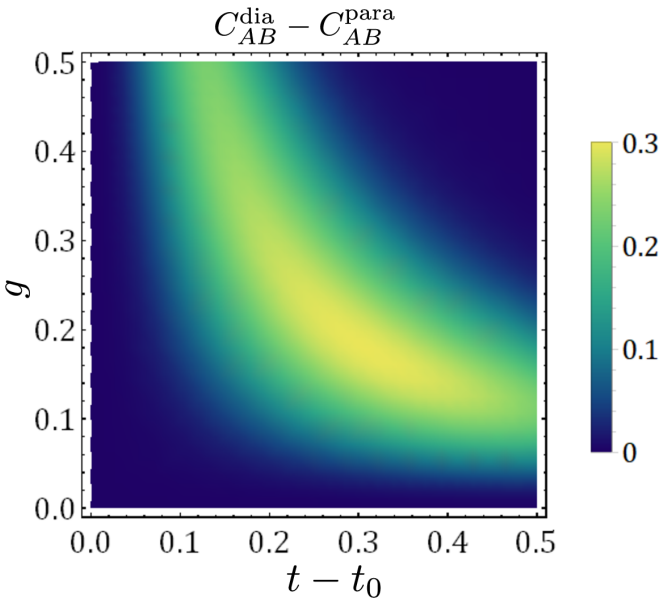

FIG. 7. Density plot vs g and $t - t_0$ for the difference between C_{AB} in the diabatic setting, with $v = 5 \times 10^{-5}$, $h_0 = 1.001$, $t_0 = \bar{t}$, and $n_d = 5$, and C_{AB} in the paramagnetic setting, with $h = 5$; $N = 1000$ in both settings.

described by a number $n_d = 2, 4, 12$ of domains, with initial values of the magnetic field $h_0 = 1.01, 1.03, 1.09$, respectively. The curves indicate that a slower quench works better, i.e., that a lower number of bigger domains (as low as just a couple) should be preferred. Referring to the time dependence of the applied field during the quench, shown in the inset of Fig. 6, we note that the slower decay of the concurrence is actually obtained in the diabatic realization where the field is closer to its critical value throughout the whole evolution. The advantage of keeping R as close as possible to the QPT might follow from the fact that condition (ii) is better fulfilled for smaller magnetization of the ring in the z direction. On the other hand, a well-known prodrome of the QPT in the static QIF is just the steep reduction of such magnetization for $h \gtrsim 1$, and we expect that a similar reduction characterizes the dynamical model (as this is necessary to allow the order parameter, i.e., the magnetization in the x direction, to become finite for $h \leqslant 1$). Therefore, the best fulfillment of condition (i), which is obtained when the ring splits into just a pair of independent domains, meets the requirement implied by point (ii) if the quench of the field keeps R as close as possible to the QPT during the whole dynamics, which explains why a slower quench of a field initially set to a lower value is seen to work better in Fig. 6.

The advantage of working well within the critical region is also appreciated in Fig. 7, where we return to the difference between the concurrence in the diabatic and the paramagnetic settings, shown as a function of g and $t - t_0$ with an initial field for the diabatic setting which is very close to the critical point, namely, $h_0 = 1.001$, and $t_0 = \bar{t}$; in this case, considerable entanglement protection is observed for an extended time interval and values of g on the order of 0.1–0.2. Note that, despite the QPT featured by the model that describes the ring being essential to ensure that the KZM occurs, the protection effect is not a critical phenomenon and can be obtained for values of the relevant parameters that do not need to be fine-tuned.

VIII. CONCLUSION

In this work we have considered a couple of qubits with a magnetic environment featuring a QPT driven by an external magnetic field. We have studied the way the entanglement between the qubits dynamically deteriorates in two different settings, namely, when the environment is kept in its disordered and paramagnetic phase by a constant field sufficiently larger than the critical one and when it is instead driven towards the critical point by linearly quenching the applied field. We have modeled the magnetic environment so that it features a KZM, with the latter setting leading to a slow diabatic evolution, characterized by the formation of uncorrelated and essentially frozen magnetic domains.

Referring to the effective description of the KZM, we have found that when the environment splits into a small number of larger domains, pointing in different directions due to their being uncorrelated, better protection of the entanglement between the two qubits is obtained. In fact, our results show that the best protection is obtained when the formation of the above domains occurs as close as possible to the critical point so as to guarantee a net magnetization of the environment in the field direction as small as possible, compatibly with the large size of the domains. It is relevant that this setting can be realized by properly choosing the initial value of the field and its quench velocity, which are indeed amenable to external control. In fact, we have described the environment as an Ising chain in a transverse field not only because this is the paradigmatic model where the KZM is known to take place, but also to relate our analysis to possible experimental studies, given that several realizations of such a model exist [36–38], with signatures of quantum critical behavior seen to persist at finite temperature [36,38–41] and recognized even for a rather small number of spins [42,43]. Moreover, experimental observations of the KZM have been recently made available via different types of quantum simulators [44–47]. Besides the results found as far as the entanglement protection between the two qubits is concerned, this work has also allowed us to obtain some analytical solutions, based on the use of spin coherent states and the Zassenhaus formula, for the quantum propagator of a composite system with a time-dependent Hamiltonian, which we believe might be useful also in different contexts.

ACKNOWLEDGMENTS

P.V. gratefully acknowledges support from the Simons Center for Geometry and Physics, Simons Foundation and Stony Brook University, where some of the research for this paper was performed. Financial support from the Università degli studi di Firenze in the framework of the University Strategic Project Program 2015 (Project Id No. BRS00215) is gratefully acknowledged. This work was done in the framework of the operating agreement between the Institute for Complex Systems of the Consiglio Nazionale delle Ricerche and the Physics and Astronomy Department of the Università degli studi di Firenze.

APPENDIX A: ZASSENHAUS FORMULA

Given two noncommuting operators $\hat{X}$ and $\hat{Y}$, the Zassenhaus formula reads

$$e^{\lambda(\hat{X}+\hat{Y})} = e^{\lambda\hat{X}} e^{\lambda\hat{Y}} e^{\lambda^2 C_2(\hat{X},\hat{Y})} \cdots e^{\lambda^n C_n(\hat{X},\hat{Y})} \cdots , \tag{A1}$$

where the operators $C_n(\hat{X},\hat{Y})$ have been recently expressed [48] as

$$C_{n+1}(\hat{X},\hat{Y}) = \frac{1}{n+1} \sum_{(i_0,\ldots,i_n)\in\mathcal{I}_n} \left[\prod_{k=0}^{n} \frac{(-1)^{i_k}}{i_k!}\right] ad_{C_n}^{i_n} \cdots ad_{C_2}^{i_2} ad_{\hat{Y}}^{i_1} ad_{\hat{X}}^{i_0} \hat{Y}, \tag{A2}$$

where

$$ad_{\hat{X}}^0 \hat{Y} = \hat{Y}, \quad ad_{\hat{X}}^k \hat{Y} = [\underbrace{\hat{X}, [\hat{X}, \ldots, [\hat{X}}_{k \text{ times}}, \hat{Y}], \ldots]], \tag{A3}$$

with $\mathcal{I}_n$ the set of $(n+1)$-tuples of non-negative integers $(i_0, i_1, \ldots, i_n)$ satisfying the conditions

$$\begin{aligned} &i_0 + i_1 + 2i_2 + \cdots + ni_n = n, \\ &k+1 \leqslant i_0 + \cdots + ki_k \; \forall\, k \leqslant n-1. \end{aligned} \tag{A4}$$

Equivalently, the left-oriented version of (A1) reads

$$e^{\lambda(\hat{X}+\hat{Y})} = \cdots e^{\lambda^n \tilde{C}_n(\hat{X},\hat{Y})} \cdots e^{\lambda^2 \tilde{C}_2(\hat{X},\hat{Y})} e^{\lambda\hat{Y}} e^{\lambda\hat{X}}, \tag{A5}$$

with $\tilde{C}_n = (-1)^{n+1} C_n$, $n \geqslant 2$.

APPENDIX B: SPIN COHERENT STATES

Spin coherent states can be introduced by following the steps given in Ref. [49]. The first step is the recognition of the dynamical group pertaining to the spin system at hand: Since the Hamiltonians in Eqs. (22) and (29) are linear functions of the operators $\{\hat{s}_i^z, \hat{s}_i^\pm\}$ and $\{\hat{S}_\delta^z, \hat{S}_\delta^\pm\}$, respectively, the group [50,51] is $G = \mathrm{SU}(2)$. The Hilbert space $\mathcal{H}_S$ associated with a spin $\mathcal{S}$, whose Hamiltonian is a linear combination of the SU(2) generators, i.e., $\{\hat{S}^z, \hat{S}^\pm\}$, is spanned by $\{|\mathcal{S}, M\rangle\}$, where $|\mathcal{S}, M\rangle$ are simultaneous eigenstates of $\hat{\mathbf{S}}^2$ and $\hat{S}^z$ (in order to simplify the notation, we omit the index i or δ throughout this Appendix, as it does not affect the construction of the spin-$\mathcal{S}$ CSs). The reference state [49] is usually taken to be the highest- or lowest-weight state of SU(2); the most natural choice is the former, i.e., $|\mathcal{S}, \mathcal{S}\rangle \equiv |0\rangle$, and this is the choice hereafter understood. The reference state identifies the maximal stability subgroup $H = \mathrm{U}(1)$, whose elements $\hat{h}$ leave $|\mathcal{S}, \mathcal{S}\rangle$ invariant up to a phase factor, according to the form $\hat{h} = e^{i\alpha\hat{S}^z}$, $\alpha \in \mathbb{R}$. The quotient group is thus $G/H = \mathrm{SU}(2)/\mathrm{U}(1)$, which is associated with the two-dimensional sphere S^2. The spin coherent states $|\Omega\rangle$ for a system with $|\hat{\mathbf{S}}|^2 = \mathcal{S}(\mathcal{S}+1)$, hereafter indicated by spin-$\mathcal{S}$CSs, are eventually defined as

$$|\Omega\rangle = \hat{\Omega}|0\rangle = e^{\Omega\hat{S}^- - \Omega^*\hat{S}^+}|0\rangle, \tag{B1}$$

where $\Omega \in \mathbb{C}$ parametrizes the sphere via

$$\Omega = \frac{\vartheta}{2} e^{i\varphi}, \tag{B2}$$

with (ϑ, φ) the polar angles and $\hat{\Omega} := \exp\{\Omega\hat{S}^- - \Omega^*\hat{S}^+\}$ the so-called displacement operator. We note that Eq. (B1), with the definition of the parameter Ω, establishes a one-to-one correspondence between the spin-$\mathcal{S}$ CSs, the elements of the quotient space G/H, and the points on the sphere, represented as normalized vectors in $\mathbb{R}^3$,

$$\hat{\Omega} \leftrightarrow \Omega \leftrightarrow \mathbf{n}(\Omega) := (\sin\vartheta\cos\varphi, \sin\vartheta\sin\varphi, \cos\vartheta). \tag{B3}$$

With the previous parametrization, the SU(2) representation of any element $\hat{\Omega} \in \mathrm{SU}(2)/\mathrm{U}(1)$ is

$$\mathbf{\Omega}(\vartheta,\varphi) = \begin{pmatrix} \cos\frac{\vartheta}{2} & -\sin\frac{\vartheta}{2} e^{-i\varphi} \\ \sin\frac{\vartheta}{2} e^{i\varphi} & \cos\frac{\vartheta}{2} \end{pmatrix}. \tag{B4}$$

As shown in Ref. [52], from the relation between the groups SO(3) and SU(2), it is possible to obtain the representation of $\hat{\Omega}$ in SO(3), which is

$$\mathbf{R}_{\Omega(\vartheta,\varphi)} = \begin{pmatrix} \cos\vartheta\cos^2\varphi + \sin^2\varphi & \sin\varphi\cos\varphi(1-\cos\vartheta) & -\sin\vartheta\cos\varphi \\ \sin\varphi\cos\varphi(1-\cos\vartheta) & \cos\vartheta\sin^2\varphi + \cos^2\varphi & \sin\vartheta\sin\varphi \\ \sin\vartheta\cos\varphi & -\sin\vartheta\sin\varphi & \cos\vartheta \end{pmatrix}. \tag{B5}$$

We recall some properties of the spin-$\mathcal{S}$ CSs which turn out to be useful in our calculation, taking a specific dimension $2\mathcal{S}+1$ of the Hilbert space. First of all, spin-$\mathcal{S}$ CSs are in general not orthogonal; in fact, they are

$$|\langle\langle\Omega'|\Omega\rangle\rangle|^2 = \left(\frac{1 + \mathbf{n}(\Omega')\cdot\mathbf{n}(\Omega)}{2}\right)^{2\mathcal{S}} = \cos^{4\mathcal{S}}\frac{\Theta}{2}, \tag{B6}$$

where $\Theta = \cos\vartheta\cos\vartheta' + \sin\vartheta\sin\vartheta'\cos(\varphi-\varphi')$. Nevertheless, the normalization of spin-$\mathcal{S}$ CSs is guaranteed, $\langle\Omega|\Omega\rangle = \langle 0|\hat{\Omega}^\dagger\hat{\Omega}|0\rangle = \langle 0|0\rangle = 1$, and the spin-$\mathcal{S}$ CSs become almost orthogonal for large $\mathcal{S}$, as $\lim_{S\to\infty} |\langle\langle\Omega'|\Omega\rangle\rangle|^2 \propto \delta(\Omega-\Omega')$. The resolution of the identity reads

$$\hat{\mathbb{I}} = \int d\mu(\Omega)|\Omega\rangle\langle\Omega| = \frac{2\mathcal{S}+1}{4\pi}\int_{\mathcal{S}^2} d\Omega|\Omega\rangle\langle\Omega|, \tag{B7}$$

where $d\Omega$ is the solid-angle volume element on $\mathcal{S}^2$, namely, $d\Omega = \sin\vartheta\, d\vartheta\, d\varphi$. Any spin-$\mathcal{S}$ CS can be expanded in the basis $\{|\mathcal{S}, M\rangle\}$,

$$|\Omega\rangle = \sum_{M=-\mathcal{S}}^{+\mathcal{S}} g_M(\Omega)|\mathcal{S}, M\rangle, \tag{B8}$$

where $g_M(\Omega) = \langle\mathcal{S}, M \,|\, \Omega\rangle$ and

$$g_M(\Omega) = \sqrt{\binom{2\mathcal{S}}{\mathcal{S}+M}} \left(\cos\frac{\vartheta}{2}\right)^{\mathcal{S}+M} \left(\sin\frac{\vartheta}{2}\right)^{\mathcal{S}-M} e^{i(\mathcal{S}-M)\varphi} \tag{B9}$$

holds.

Finally, the composition law for different displacement operators is needed. To this aim, let us consider the operators

$\hat{\Omega}_1$ and $\hat{\Omega}_2$, which are associated with the unit vectors on the sphere $\mathbf{n}(\Omega_1)$ and $\mathbf{n}(\Omega_2)$, respectively,

$$\hat{\Omega}_1\hat{\Omega}_2 = \hat{\Omega}_3 e^{-i\Phi(\Omega_1,\Omega_2)\hat{S}^z}, \tag{B10}$$

where $\hat{\Omega}_3$ is associated with the unit vector $\mathbf{n}(\Omega_3)$, obtained from $\mathbf{n}(\Omega_2)$ after the rotation $\mathbf{R}_{\Omega_1} \in \mathrm{SO}(3)$ induced by the operator $\hat{\Omega}_1$, i.e.,

$$\mathbf{n}(\Omega_3) = \mathbf{R}_{\Omega_1}\mathbf{n}(\Omega_2), \tag{B11}$$

meaning that a displacement operator $\hat{\Omega}$ transforms any spin-$\mathcal{S}$CS $|\Omega'\rangle$ into another spin-$\mathcal{S}$ CS, up to a phase factor.

APPENDIX C: INITIAL STATE OF DOMAINS IN THE DIABATIC CASE

The initial state of the ring in the diabatic region in Eqs. (30) and (31) describes each domain pointing in some direction $\mathbf{n}_\delta(0) := \mathbf{n}(\vartheta_\delta(0), \varphi_\delta(0))$, where the spherical polar angles $(\vartheta_\delta(0), \varphi_\delta(0))$ identify a point on a sphere. Referring to the strategy for choosing the initial conditions, it is worth saying that the lack of correlations among domains will allow for an independent choice of $(\vartheta_\delta(0), \varphi_\delta(0))$.

Nevertheless, their values have to be related to the phenomenology of the KZM in the diabatic region. Indeed, we must properly take into account that the magnetization of each domain is proportional to the expectation value of the operator $\hat{\mathbf{S}}_\delta$ on the state of the δth domain, averaged on different possible configurations $\mathbf{M}_\delta(t) = \langle\hat{\mathbf{S}}_\delta\rangle$, where the time dependence of magnetization is due to the time evolution of the state of each domain.

The choice of $\vartheta_\delta(0)$ is related to the value $h_0 \equiv h(t_0)$ of the external magnetic field at the time t_0 (the time when the two-qubit system starts to evolve after having been prepared in a well-defined initial state), within the diabatic region. In fact, since $\vartheta_\delta(0)$ represents the angle between the unit vector $\mathbf{n}_\delta$ defined by the pair $(\vartheta_\delta, \varphi_\delta)$ and the z axes, then $\vartheta_\delta(0)$ determines the magnetization of the δth domain along the z direction. We thus select each $\vartheta_\delta(0)$ in such a way that the average magnetization of the entire ring is equal to nm_0^z, where m_0^z is the equilibrium average magnetization per particle of the ring for the chosen value h_0 of the external field, as given by Ref. [53].

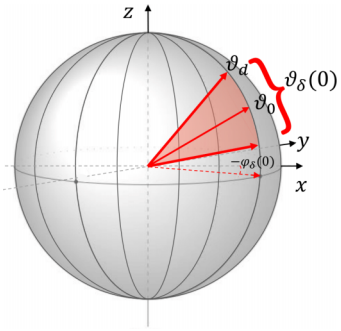

FIG. 8. Schematic representation of the selection process for the initial point $(\vartheta_\delta(0), \varphi_\delta(0))$.

The selection proceeds as follows. We start by choosing a domain δ_1 and we select the corresponding $\cos[\vartheta_{\delta_1}(0)] \equiv m^z_{\delta_1}$ from a uniform distribution centered on m_0^z and having width $\Delta_0 = |m_d^z - m_0^z|$, with m_d^z the magnetization corresponding to the value $h_d = h(\bar{t})$ of the external field when the ring enters the diabatic region. We then move to another domain δ_2 and we select the corresponding $\cos[\vartheta_{\delta_2}(0)]$ from a uniform distribution centered on $m_1^z = (n\,m_0^z - m^z_{\delta_1})/(n-1)$ and having width $\Delta_1 = \min(|m_d^z - m_1^z|, |m_0^z - \Delta_0 - m_1^z|)$ and so on up to the last $\vartheta_{\delta_n}(0)$. The selection process of $\vartheta_{\delta_1}(0)$ is sketched in Fig. 8, where ϑ_0 and ϑ_d are defined such that $\cos(\vartheta_0) = m_0$ and $\cos(\vartheta_d) = m_d$.

It is worth noting that the choice of such an initial condition allows us to distinguish different time instants in the diabatic region, due to the dependence of the z magnetization on the external magnetic field. As for $\varphi_\delta(0)$, i.e., the angle between the projection of the unit vector $\mathbf{n}_\delta$ on the x-y plane and the x axes, we have to refer to the magnetization in the x direction, which is the order parameter of the model. Since we are preparing the ring in the disordered region, we choose each $\varphi_\delta(0)$ to assume randomly the value 0 or π so that the x magnetization of each domain can be aligned in the direction $+x$ or $-x$ with the same probability.

[1] H. Breuer and F. Petruccione, *The Theory of Open Quantum Systems* (Oxford University Press, Oxford, 2002).

[2] A. Rivas and S. F. Huelga, *Open Quantum Systems* (Springer, Berlin, 2012).

[3] R. L. Franco, New J. Phys. **17**, 081004 (2015).

[4] C. P. Koch, J. Phys.: Condens. Matter **28**, 213001 (2016).

[5] S. N. A. Duffus, V. M. Dwyer, and M. J. Everitt, Phys. Rev. B **96**, 134520 (2017).

[6] T. Bullock, F. Cosco, M. Haddara, S. H. Raja, O. Kerppo, L. Leppäjärvi, O. Siltanen, N. W. Talarico, A. De Pasquale, V. Giovannetti, and S. Maniscalco, Phys. Rev. A **98**, 042301 (2018).

[7] G. L. Giorgi, F. Plastina, G. Francica, and R. Zambrini, Phys. Rev. A **88**, 042115 (2013).

[8] E. Vicari, Phys. Rev. A **98**, 052127 (2018).

[9] B. Bellomo, A. D. Pasquale, G. Gualdi, and U. Marzolino, J. Phys. A: Math. Theor. **43**, 395303 (2010).

[10] R. Lo Franco, A. D'Arrigo, G. Falci, G. Compagno, and E. Paladino, Phys. Rev. B **90**, 054304 (2014).

[11] J. F. Poyatos, J. I. Cirac, and P. Zoller, Phys. Rev. Lett. **77**, 4728 (1996).

[12] S. Diehl, A. Micheli, A. Kantian, B. Kraus, H. Büchler, and P. Zoller, Nat. Phys. **4**, 878 (2008).

[13] M. J. Kastoryano, F. Reiter, and A. S. Sørensen, Phys. Rev. Lett. **106**, 090502 (2011).

[14] M. Rafiee, C. Lupo, H. Mokhtari, and S. Mancini, Phys. Rev. A **85**, 042320 (2012).

[15] M. B. Plenio and S. F. Huelga, Phys. Rev. Lett. **88**, 197901 (2002).

[16] S. Clark, A. Peng, M. Gu, and S. Parkins, Phys. Rev. Lett. **91**, 177901 (2003).

[17] L. Hartmann, W. Dür, and H.-J. Briegel, Phys. Rev. A **74**, 052304 (2006).
[18] M. Rafiee, A. Nourmandipour, and S. Mancini, Phys. Rev. A **94**, 012310 (2016).
[19] S. Mancini and J. Wang, Eur. Phys. J. D **32**, 257 (2005).
[20] L.-T. Shen, X.-Y. Chen, Z.-B. Yang, H.-Z. Wu, and S.-B. Zheng, Phys. Rev. A **84**, 064302 (2011).
[21] P.-B. Li, S.-Y. Gao, H.-R. Li, S.-L. Ma, and F.-L. Li, Phys. Rev. A **85**, 042306 (2012).
[22] E. Fiorelli, A. Cuccoli, and P. Verrucchi, Proceedings **12**, 10 (2019).
[23] E. H. Lieb, Commun. Math. Phys. **31**, 327 (1973).
[24] S. Sachdev, *Quantum Phase Transitions*, 2nd ed. (Cambridge University Press, Cambridge, 2011).
[25] T. W. B. Kibble, J. Phys. A: Math. Gen. **9**, 1387 (1976).
[26] W. H. Zurek, Nature (London) **317**, 505 (1985).
[27] W. Zurek, Phys. Rep. **276**, 177 (1996).
[28] W. H. Zurek, U. Dorner, and P. Zoller, Phys. Rev. Lett. **95**, 105701 (2005).
[29] J. Dziarmaga, Phys. Rev. Lett. **95**, 245701 (2005).
[30] J. Dziarmaga, Adv. Phys. **59**, 1063 (2010).
[31] A. Del Campo and W. H. Zurek, Int. J. Mod. Phys. A **29**, 1430018 (2014).
[32] P. Silvi, G. Morigi, T. Calarco, and S. Montangero, Phys. Rev. Lett. **116**, 225701 (2016).
[33] A. Fubini, G. Falci, and A. Osterloh, New J. Phys. **9**, 134 (2007).
[34] W. K. Wootters, Phys. Rev. Lett. **80**, 2245 (1998).
[35] H. Zassenhaus, Abh. Math. Sem. Hamburg **13**, 1 (1939).
[36] R. Coldea, D. A. Tennant, E. M. Wheeler, E. Wawrzynska, D. Prabhakaran, M. Telling, K. Habicht, P. Smeibidl, and K. Kiefer, Science **327**, 177 (2010).
[37] S. Suzuki, J.-i. Inoue, and B. K. Chakrabarti, *Quantum Ising Phases and Transitions in Transverse Ising Models* (Springer, Berlin, 2013).
[38] T. Liang, S. M. Koohpayeh, J. W. Krizan, T. M. McQueen, R. J. Cava, and N. P. Ong, Nat. Commun. **6**, 7611 (2015).
[39] A. Bayat, T. J. G. Apollaro, S. Paganelli, G. De Chiara, H. Johannesson, S. Bose, and P. Sodano, Phys. Rev. B **93**, 201106(R) (2016).
[40] S. Campbell, M. J. M. Power, and G. De Chiara, Eur. Phys. J. D **71**, 206 (2017).
[41] T. Fogarty, A. Usui, T. Busch, A. Silva, and J. Goold, New J. Phys. **19**, 113018 (2017).
[42] A. Orieux, J. Boutari, M. Barbieri, M. Paternostro, and P. Mataloni, Sci. Rep. **4**, 7184 (2014).
[43] P. Xue, X. Zhan, and Z. Bian, Sci. Rep. **7**, 2183 (2017).
[44] K. Pyka, J. Keller, H. Partner, R. Nigmatullin, T. Burgermeister, D. Meier, K. Kuhlmann, A. Retzker, M. Plenio, W. Zurek, A. del Campo, and T. Mehlstäubler, Nat. Commun. **4**, 2291 (2013).
[45] M. Anquez, B. A. Robbins, H. M. Bharath, M. Boguslawski, T. M. Hoang, and M. S. Chapman, Phys. Rev. Lett. **116**, 155301 (2016).
[46] J.-M. Cui, Y.-F. Huang, Z. Wang, D.-Y. Cao, K. Wang, W.-M. Lv, L. Luo, A. del Campo, Y.-J. Han, C.-F. Li, and G.-C. Guo, Sci. Rep. **6**, 33381 (2016).
[47] A. Keesling, A. Omran, H. Levine, H. Bernien, H. Pichler, S. Choi, R. Samajdar, S. Schwartz, P. Silvi, S. Sachdev, P. Zoller, M. Endres, M. Greiner, V. Vuletić, and M. Lukin, Nature (London) **568**, 207 (2019).
[48] F. Casas, A. Murua, and M. Nadinic, Comput. Phys. Commun. **183**, 2386 (2012).
[49] W.-M. Zhang, D. H. Feng, and R. Gilmore, Rev. Mod. Phys. **62**, 867 (1990).
[50] R. Gilmore, Ann. Phys. (NY) **74**, 391 (1972).
[51] A. M. Perelomov, Commun. Math. Phys. **26**, 222 (1972).
[52] M. Combescure and D. Robert, *Coherent States and Applications in Mathematical Physics* (Springer Science + Business Media, New York, 2012).
[53] P. Pfeuty, Ann. Phys. (NY) **57**, 79 (1970).